

# Radioimaging Evaluation of Primary Bone Tumors and Tumor like Lesions

Sunil K Vatukiya<sup>1</sup>, Bhautik Kapadia<sup>2</sup>

<sup>1</sup>Post Graduate Student, Department of Radiodiagnosis, Sir Sayajirao General Hospital and Medical College, Vadodara, Gujarat, India, <sup>2</sup>Associate Professor, Department of Radiodiagnosis, Sir Sayajirao General Hospital and Medical College, Vadodara, Gujarat, India.

## Abstract

**Background:** Bone tumour is relatively rarely encountered by radiologist, so sometimes it creates diagnostic difficulty. Aim over study was to determine the X-ray CT and MRI characteristics of different primary bone tumours and tumour like lesion and correlation of radiologic diagnosis with histopathologic diagnosis whenever possible. To understand the advantages and limitations of different radio-imaging techniques. **Subjects and Methods:** We have studied total 45 cases of primary bone tumour and tumour like lesions during study of 15 months duration in department of Radiodiagnosis, Baroda Medical College, Vadodara, Gujarat, India. First radiological diagnosis and differential diagnosis was given than histopathologic examination was done in all malignant and indeterminate lesions for final diagnosis. **Results:** Out of 45 patients 21 (46.6%) were female and 24 (53.3%) were male. Benign and malignant lesions were 69% and 31% respectively. Multiple lesions were common with osteochondroma, hemangioma and multiple myeloma. Most common malignant tumour was osteosarcoma and benign tumour was osteochondroma. Pathologic fracture was seen in 6 patients but out of them 2 fractures were missed on radiograph. Skip lesions were seen in two malignant lesions which was missed on radiograph and CT but it was easily detected on MRI. **Conclusion:** Radiography is baseline investigation for evaluation of bone tumor and tumour like lesions. Pathological fracture and matrix mineralization can be better seen on CT. MR is superior in detection skip lesion, soft tissue and marrow extension.

**Keywords:** Bone tumour, X ray, CT, MRI.

**Corresponding Author:** Bhautik Kapadia, Associate Professor, Department of Radiodiagnosis, Sir Sayajirao General Hospital and Medical College, Vadodara, Gujarat, India.

E-mail: [drbhautikkapadia@gmail.com](mailto:drbhautikkapadia@gmail.com)

Received: 06 January 2020

Revised: 05 February 2020

Accepted: 20 February 2020

Published: 05 July 2020

## Introduction

The development of more effective chemotherapeutic agents, combined with improvements in limb salvage surgery and advances in imaging technology, has resulted in improved staging and ultimate outcome in patients with these bone and soft-tissue lesions.

Plain radiographs are an indispensable part of the diagnostic evaluation of the patients with any skeletal symptoms and signs, and remains the first and foremost imaging modality. Plain radiograph is a cheap, sensitive and easily available imaging tool and has high cost-benefit ratio.

However, plain radiograph is a two dimensional representation of a three dimensional body part; and hence carries inherently low spatial resolution and overlapping of structures. Moreover, plain radiograph has limited role in evaluation of the marrow and soft tissues, for which CT scan and preferably MRI are more advantageous.

In current scenario, Patient with skeletomuscular symptoms, the provisional diagnosis regarding the presence and type of the bone tumour is usually made by a plain radiograph. For further characterization and extension of the lesion CT scan or MRI is used.

Radiology provides the idea about the gross pathoanatomy about the lesion, whereas the biopsy represents only a part of the lesion. Thus, in most of the cases the radiology provides the first idea about the diagnosis, & the histology confirms the final diagnosis. So good communication and cooperation is required between the clinician, radiologist & a pathologist in management of patient with bone lesions.

This study will describe how X-ray, CT and MR is useful in diagnosis and characterization of different bone tumors. [1-4]

## Subjects and Methods

This was prospective study of 45 patients with bone lesions referred from orthopedic department for radiograph, CT scan and MRI study in department of Radiodiagnosis in sir sayajirao general hospital and medical college- Vadodara. This study includes clinical, radiographic, CT and MRI findings of patients with bone tumour and tumour like lesions. Institutional ethics committee has approved the study and informed written consent was taken from parents. All patients were evaluated with plain radiograph by taking at least two projections. After that CT and MRI study was performed. CT was performed by using 16 slice multi-detector spiral CT machine of General Electric. Axial as well as coronal and sagittal reconstructed CT images were acquire and evaluated. MRI was performed by using GE 1.5 TESLA Electro magnet at sahyog imaging center, medical college Vadodara. First T1W FSE and PDFS sequences with large field of view are obtained to localize area of interest using body coil. After that T1, PDFS, gradient and STIR sequences are obtained using surface coil. Post contrast T1 weighted fat saturated MR images were obtained after administration of gadolinium (0.1 mmol/kg body weight).

Bone tumours were categorized according to age group, benign or malignant, involved bone, number of lesions, pattern of bone destruction and type of matrix mineralization. Data were analyzed in percentage and proportions by Microsoft excel.

## Results

Total 45 patients of primary bone tumour and tumour like lesion were studied using radiography, CT and/or MRI. Out of them 21(46.6%) were female and 24(53.3%) were male. Majority of them presented with nonspecific complains of pain and swelling over local site. Most common bone involved was femur followed by tibia. Few of the lesion like osteochondroma, hemangioma and multiple myeloma showed multiple lesions.

Benign lesions constituted 69% of cases (n = 31), whereas malignant lesions constituted 31% of cases (n = 14).

Overall, the commonest tumour was found to be osteosarcoma (17% cases; n = 8), followed in descending order of frequency by osteochondroma (15% cases; n = 7) and non-ossifying fibroma (n = 5, 11% cases).

Out of malignant tumour most common malignant tumour was osteosarcoma (57% cases; n = 8), followed by multiple myeloma (14% cases; n = 2) and Ewing sarcoma (14% cases; n = 2).

Out of benign tumour most common benign tumour was osteochondroma (22%; n=7) followed by non-ossifying fibroma

Table 1: Age wise distribution of lesions

Diagnosis	Age Group			Total
	≤20	21-40	>40	
Enchondroma	0	3	0	3
Ewing Sarcoma	2	0	0	2
Ossifying fibroma	0	1	0	1
Osteoma	0	1	0	1
Benign fibrous histiocytoma	0	0	1	1
Chondrosarcoma	0	0	1	1
Osteosarcoma	6	0	2	8
Giant cell tumour	0	2	1	3
Osteochondroma	3	3	1	7
Simple bone cyst	1	1	2	4
Multiple myeloma	0	0	2	2
Non ossifying fibroma	3	2	0	5
Malignant giant cell tumour	1	0	0	1
Aneurysmal bone cyst	2	0	0	2
Odontogenic keratocyst	0	1	0	1
Osteoid Osteoma	0	1	0	1
Hemangioma	0	0	1	1
Ameloblastoma	0	0	1	1
Total	18	15	12	45

(16%; n=5), enchondroma (9%; n=3).

All the benign lesions had well defined margins with marrow zone of transition, whereas all the malignant lesions had ill-defined margins with wide zone of transition except lesion of multiple myeloma in skull showed well defined margin with narrow zone of transition.

Six lesions (13% of cases) had pathological fracture. Out of these, two pathological fractures were missed on plain radiographs and were detected on CT and MRI scan.

Pattern of matrix mineralization was evaluated on both plain radiography and on CT scan. In 2 cases plain radiograph could

not detect right matrix. Out of these two case one was of ossifying fibroma of right maxillary sinus and chondrosarcoma of metacarpal.

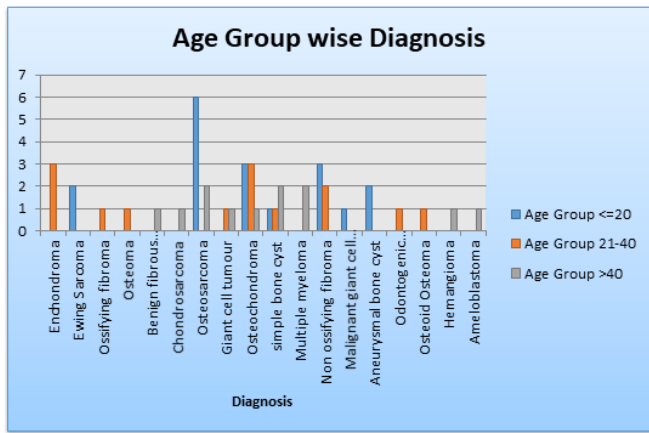


Table 2: Nature of Lesion & Periosteal Reaction

Nature of	Periosteal Reaction		Total
	Yes	No	
Malignant	9(64.28%)	5(35.72%)	14
Benign	0(0%)	31(100%)	31

Table 3: Nature of Lesion & Pattern of Destruction

Nature	Pattern of Destruction			Total
	Geographi N (%)	Permeativ N (%)	Moth Eaten N (%)	
Malignant	3 (21.43)	2 (14.29)	9 (64.29)	14
Benign	31 (100.00)	0 (0.00)	0 (0.00)	31
Total	34 (75.00)	2 (4.55)	9 (20.45)	45

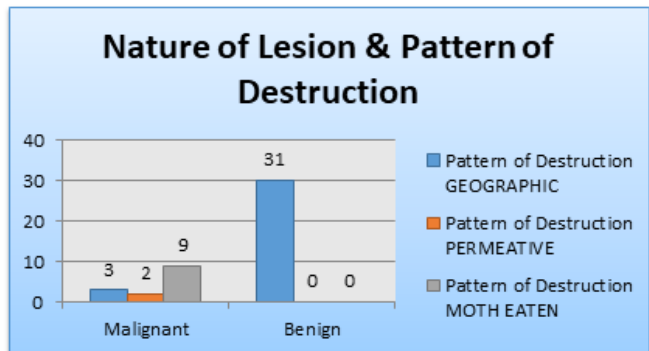


Table 4: Nature of Lesion & Zone of Transition

Nature of	Zone of Transition		Total
	Narrow N (%)	Wide N (%)	
Malignant	2 (14.29)	12 (85.71)	14
Benign	31 (100.00)	0 (0.00)	31
Total	33 (72.73)	12 (27.27)	45

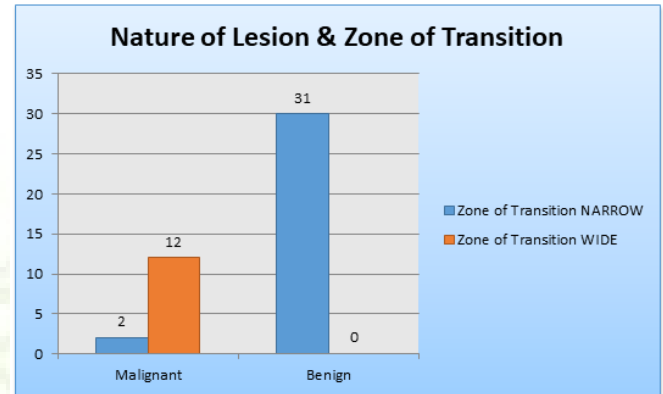


Table 5: Types of Bone involved

Types of Bone	No. of Diagnosis	Percentage
Rib	1	2.22
Femur	12	26.6
Maxilla	1	2.22
Temporal	1	2.22
Tibia	10	22.2
Metacarpals	2	4.44
Fibula	3	6.66
Humerus	2	4.44
Skull, Rib, Vertebra	1	2.22
Clavicle	1	2.22
Phalanges	1	2.22
Multiple Bones	5	11.11
Mandible	2	4.44
Ulna	1	2.22
Talus	1	2.22
Radius	1	2.22
Total	45	100.00

**Cases discussion**

**Case 1:** A 35 years old female with c/o headache following trauma.

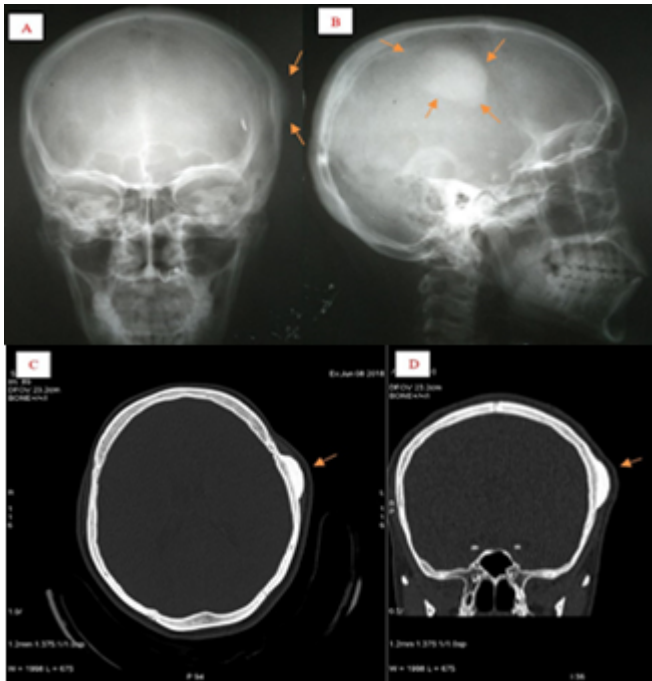


Figure 1: (A) X ray skull AP and (B) lateral view, (C,D) axial and coronal CT images of head, bone window showing well defined exophytic densely sclerotic lesion (orange arrow) with narrow zone of transition arising from left parietal bone.

**Radiologic diagnosis: Osteoma of skull**

**Case-2:** 25 years old male with c/o swelling over right lower antero-lateral chest wall.

**Radiologic diagnosis:** Enchondroma of right 7th rib

**Histopathologic diagnosis:** Enchondroma of right 7th rib

**Case 3:** A 15 years old female with c/o left wrist pain following trauma.

**Radiologic diagnosis:** Non ossifying fibroma of left radius

**Case 4:** 25 years old male with c/o pain over right ankle following trauma.

**Radiologic diagnosis:** Simple bone cyst with pathologic fracture of talus Simple bone cyst are usually painless. It show periosteal reaction only if pathologic fracture.<sup>[5]</sup>

**Case 5:** A 25 years old female with c/o right knee pain following trauma.

**Radiologic diagnosis:** Fibrous cortical defect of right proximal tibia



Figure 2: X-ray of chest with zoomed image showing well defined expansile osteolytic lesion (orange arrow) with narrow zone of transition without visible matrix within involving anterior aspect of right 7<sup>th</sup> rib.

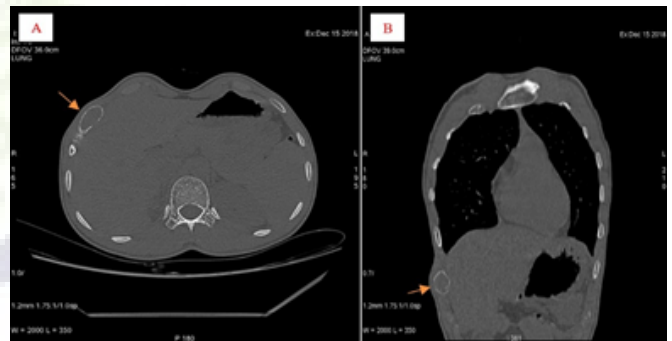


Figure 3: (A) axial and (B) coronal CT bone window image showing well defined expansile osteolytic lesion (orange arrow) with narrow zone of transition without matrix mineralization within involving anterior aspect of right 7th rib.

**Case 6:** A 35 years old female with c/o right knee pain.

**Radiologic diagnosis:** Giant cell tumour of right distal femur pathological fracture

**Histopathologic diagnosis:** Giant cell tumour

Giant cell tumour is seen after 30 years of age however few cases are reported before 30 years. It does not show sclerotic rim.<sup>[6]</sup>

Chondromyxoid fibroma and benign fibrous histiocytoma can be considered as deferential diagnosis of giant cell tumour. Chondromyxoid fibroma is seen before 30 years of age. It is also seen in epi-metaphysis however it shows peripheral sclerotic rim.<sup>[7]</sup> Benign fibrous histiocytoma is seen after 30 years. It is medullary lesion with complete or partial

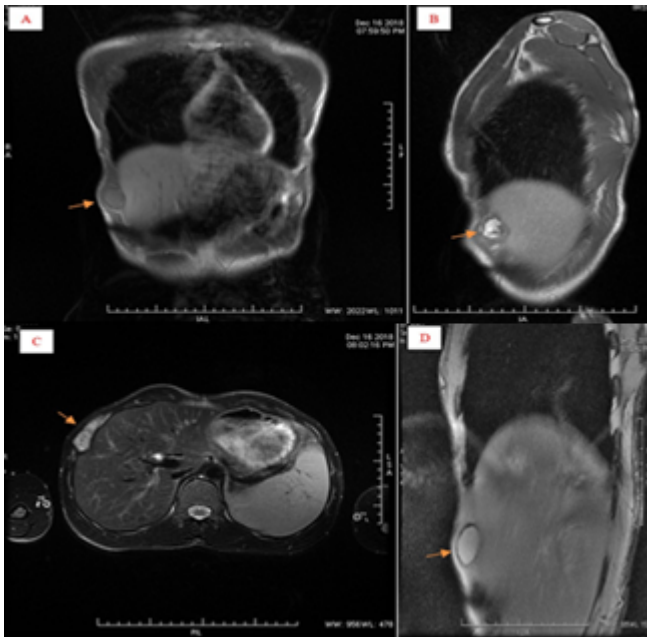


Figure 4: (A) Coronal T1, (B) sagittal T2, (C) axial STIR and (D) gradient MR sequence showing well defined expansile abnormal marrow signal intensity lesion-hypointense on T1, hyperintense on T2 and STIR without blooming on gradient image involving anterior aspect of right 7th rib. No evidence of hemorrhagic layering.

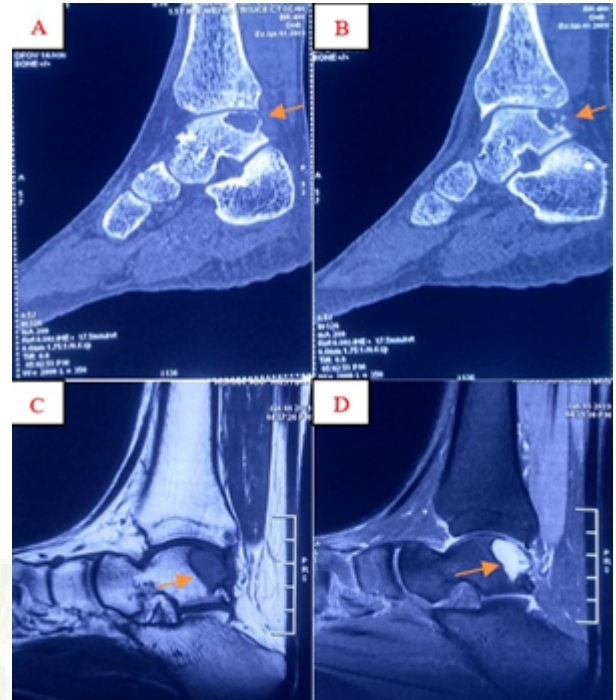


Figure 6: (A,B) CT scan of ankle sagittal image, showing well defined osteolytic lesion (orange arrow) with fractured bone fragment within (Fallen fragment sign) seen involving talus. (C,D) MRI ankle of same patient, sagittal T1 weighted (left) and PDFS (right) images- Lesion in talus appears hypointense on T1 weighted image and hyperintense with fluid-fluid level, secondary to fracture on PDFS images.



Figure 5: X-ray left wrist lateral and AP views showing well defined expansile, lobulated, osteolytic lesion with narrow zone of transition with ground glass matrix and thin peripheral sclerotic rim involving medial cortex of metaphysis of left distal wrist.

peripheral sclerotic rim involving epi-metaphysis with ground glass matrix mineralization. [8-10]

Brown's tumour of hyperparathyroidism is always a differential diagnosis of giant cell tumour however it present with other radiographic manifestation of hyperparathyroidism and raised parathormone level. [9]

**Case 7:** A 7 years old female child with c/o swelling over right knee.

**Radiologic diagnosis:** Aneurysmal bone cyst of right distal femur

**Case 8:** A 19 years old male with c/o swelling over left knee.

**Radiologic diagnosis:** Aneurysmal bone cyst of left femur

**Case 9:** A 55 years old female with complaint of knee pain

**Radiological differential diagnosis:** Giant cell tumour, benign fibrous histiocytoma, chondromyxoid fibroma, brown's tumour of hyperparathyroidism

**Histopathologic diagnosis:** Benign fibrous histiocytoma



Figure 7: (A) X-ray right knee with proximal leg AP and lateral view, (B,C) CT axial and sagittal bone window showing well defined eccentric osteolytic lesion (orange arrow) with typical ground glass matrix and peripheral sclerotic rim abutting posterior cortex of tibia.

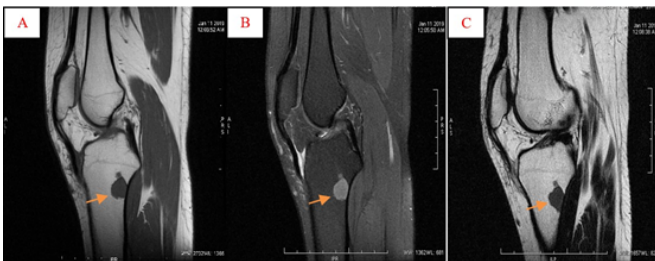


Figure 8: (A) Sagittal T1, (B) PDFS and (C) T2 weighted MR image of same patient showing well defined eccentric abnormal marrow signal intensity lesion- hypointense on T1 and T2 weighted images and hyperintense on PDFS image abutting posterior cortex of proximal tibia.

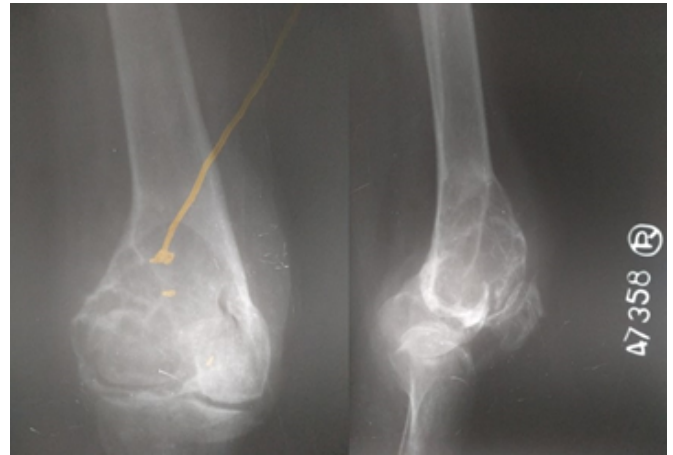


Figure 9: X-ray right knee AP and lateral views showing well defined expansile, eccentric, lobulated, osteolytic lesion with narrow zone of transition without visible matrix. No peripheral sclerotic rim; involving epimetaphysis of right distal femur, extending upto articular surface.

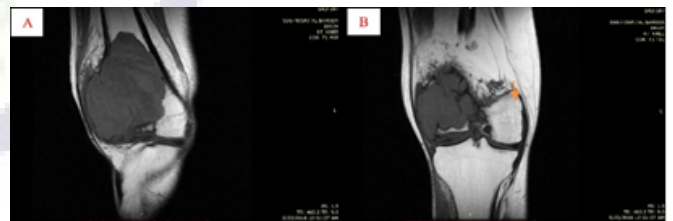


Figure 10: (A,B) coronal T1 weighted MR image showing well defined eccentric abnormal marrow signal intensity lesion appearing heterogeneously hypointense involving epimetaphysis of right distal femur. Note the displaced fracture (orange arrow) of right femoral condyle with intra-articular extension.

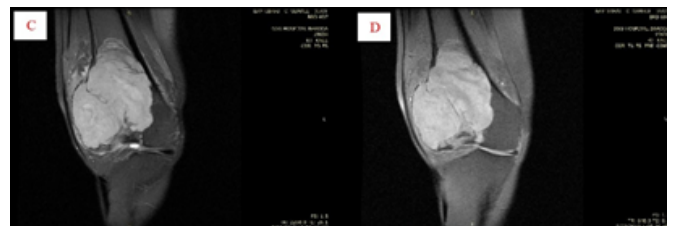


Figure 11: (C) coronal PDFS and (D) T1 post contrast fat saturated MR images, it appears hyperintense on PDFS and moderate heterogeneous enhancement after administration of gadolinium.

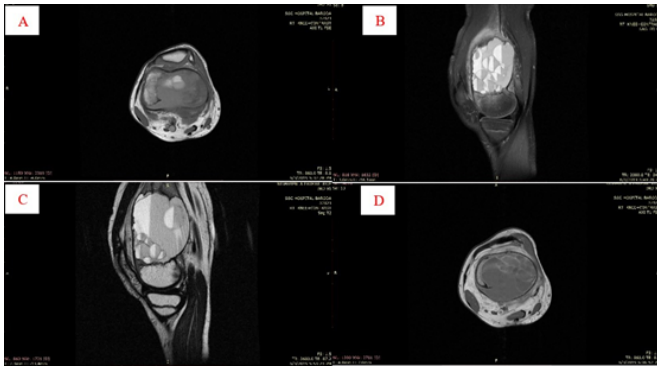


Figure 12: MRI of knee showing expansile, eccentric abnormal marrow signal intensity lesion in distal femoral metaphysis. It appears hypointense with few hyperintense area within on T1 weighted image (A), variable areas of iso and hyperintensity making fluid-fluid level on PDSEF and T2 weighted image (B,C) with enhancement on septations in T1 post contrast image (D).

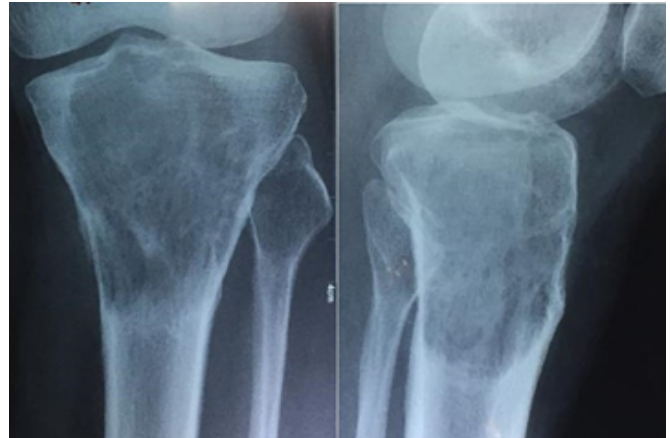


Figure 14: X-ray left knee AP and lateral views showing well defined expansile, eccentric osteolytic lesion with narrow zone of transition with ground glass matrix involving epimetaphysis of left proximal tibia.

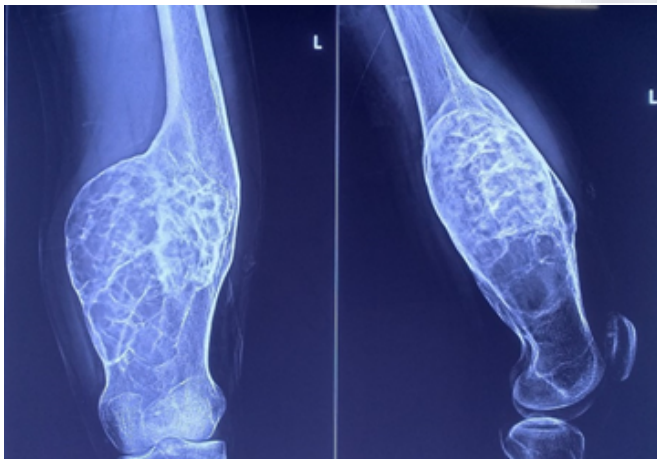


Figure 13: X-ray left knee AP and lateral views showing well defined expansile, eccentric, lobulated, osteolytic lesion with narrow zone of transition without visible matrix with peripheral thin sclerotic rim; involving diaphysis of right distal femur. Note the epiphysis and physis appear normal.



Figure 15: MRI of knee showing expansile, eccentric abnormal marrow signal intensity lesion in proximal tibial epimetaphysis. It shows homogeneously intermediate signal on T1 weighted images (A,B) and homogeneously hyperintense to skeletal muscle on PDSEF (C,D) and T2 weighted (E,F) images. Hyperintensity on PDSEF images is seen in muscles adjacent to lesion over posterior aspect possibly represents edema. No evidence of cortical break or pathological fracture.

Benign fibrous histiocytoma shows complete or partial sclerotic rim that can help in differentiating it from giant cell tumour however it is not seen in our case. [10]

**Case 10:** A 65 years old male with c/o swelling over left hip, h/o similar complaint in brother.



**Figure 16:** (A) X-ray pelvis with both hip AP view), (B, D) bilateral elbow with forearm AP and lateral view, (C, E) bilateral ankle with distal leg AP and lateral view and (F) bilateral knee AP view showing multiple sessile and pedunculated bony outgrowths arising from metaphyses of bilateral proximal and distal femora, tibia and fibulae. Note shortening and bowing of bilateral ulna (Bayonet deformity) as well as widening of bilateral femoral, tibial and fibular metaphysis (Erlenmeyer flask deformity).

**Radiological diagnosis:** Diaphyseal aclasis/Multiple hereditary exostosis

**Case 11:** A 23 years old male with c/o swelling over right mandibular region.

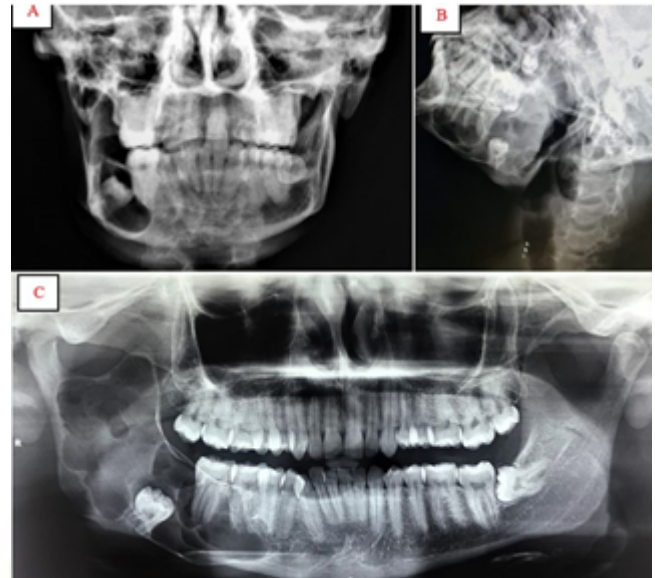


**Figure 17:** X-ray mandible (A) AP and (B) oblique view and (C) orthopantomogram showing well defined multilobulated expansile osteolytic lesion with thin peripheral sclerotic rim involving body and ramus of right side of mandible. Note the impacted molar tooth within the lesion.

**Radiological differential diagnosis:** Ameloblastoma, odontogenic keratocyst, aneurysmal bone cyst.

**Histopathologic diagnosis:** Odontogenic keratocyst.

Odontogenic keratocyst are more likely to show aggressive growth pattern than other odontogenic lesions and may show multilocular appearance; this characteristics make odontogenic cyst indistinguishable from ameloblastoma. [11]

**Case 12:** A 30 years old male with c/o pain over right forearm.

**Radiologic diagnosis:** Osteoid osteoma of right distal ulna

High resolution CT is investigation of choice for detection of radioleucant nidus of osteoid osteoma. [2]

**Case 13:** A 49 years old male with c/o swelling over mandibular region on right side.

**Radiologic diagnosis:** Ameloblastoma of mandible

**Histologic diagnosis:** Ameloblastoma

**Case 14:** A 60 years old female with c/o left periorbital and frontal swelling.

**Radiologic diagnosis:** Hemangioma

**Histopathologic diagnosis:** Cavernous hemangioma

**Case 15:** A 40 years female with c/o right maxillary swelling.



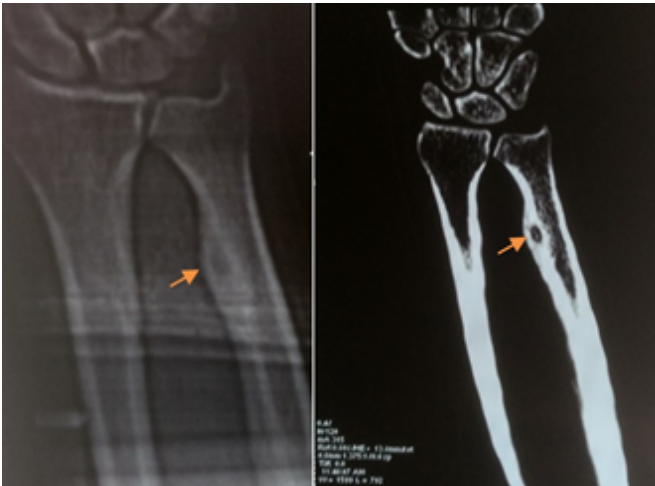


Figure 18: X-ray right forearm AP view (left) and coronal CT bone window image (right) of forearm showing well defined sclerotic lesion with radiolucent center with solid periosteal reaction involving lateral cortex of right distal ulna. Note the nidus of osteoid osteoma is better seen on CT.

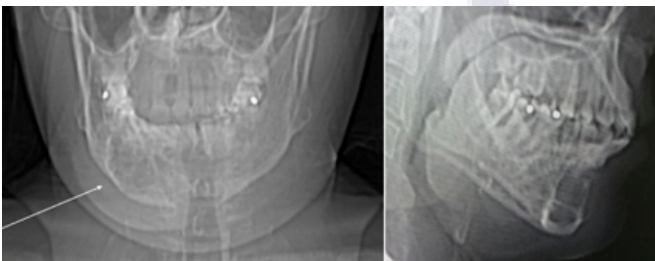


Figure 19: X-ray mandible AP and lateral view showing ill-defined expansile, lobulated osteolytic lesion (white arrow) involving anterior and right lateral aspect of body of mandible.

**Radiologic differential diagnosis:** Giant cell granuloma, Ossifying fibroma

**Histopathologic diagnosis:** Ossifying fibroma

**Case 16:** A 14 years female with c/o pain and swelling over left distal leg.

**Radiologic differential diagnosis:** Malignant giant cell tumour, telangiectatic osteosarcoma and aneurysmal bone cyst.

**Histopathologic diagnosis:** Malignant giant cell tumour

**Case 17:** A 20 years old male with c/o pain and swelling over left distal leg and ankle.

**Radiologic diagnosis:** Osteosarcoma of left distal tibia

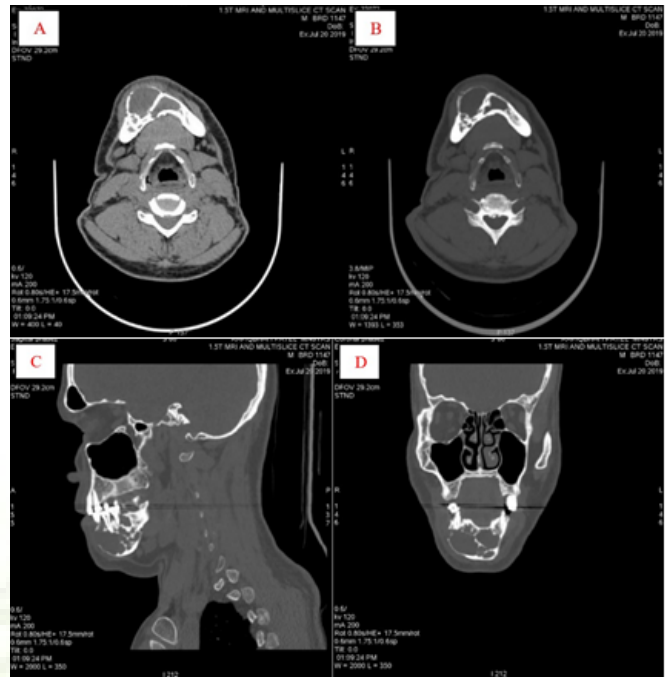


Figure 20: (A) axial CT soft tissue window and (B,C,D) axial, sagittal and coronal bone window images showing multilobulated expansile osteolytic lesion giving soap bubble like appearance seen in body of mandible with resorption of adjacent teeth and root blunting. Note severe cortical thinning. Possible radiologic diagnosis is Ameloblastoma which was proved on histopathology.

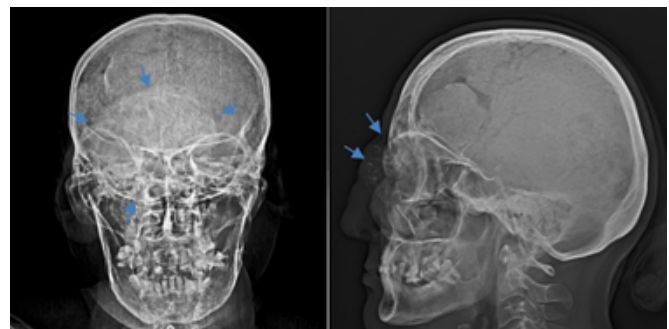


Figure 21: X-ray skull AP and lateral view showing expansile osteolytic lesion with bony striations (blue arrows) within involving frontal, ethmoid and nasal bones.



Figure 22: (A) sagittal and (B) axial CT images, bone window showing soft tissue density mass lesion causing osteolysis of frontal, ethmoid and nasal bones with bony striations within. It extending into the nasal cavity. On MR (C) axial T1 weighted image the lesion appears hypointense, (D) on axial T2 weighted image it appear hyperintense and shows strong heterogeneous enhancement after administration of gadolinium (E).

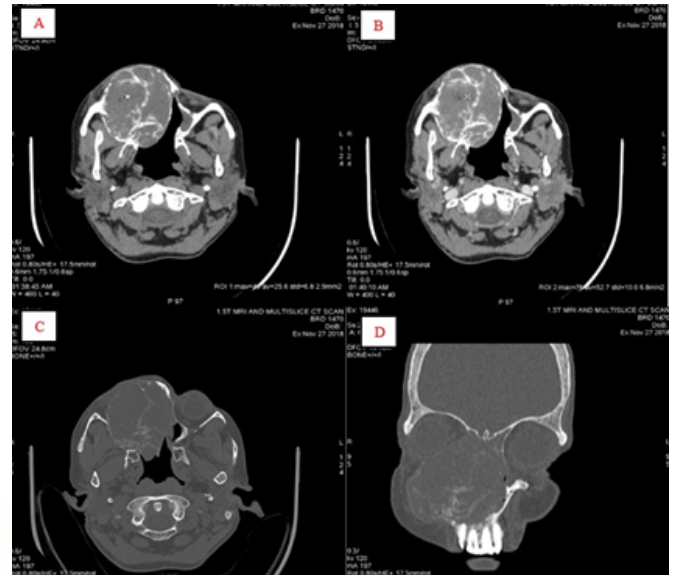


Figure 24: (A) axial CT soft tissue window pre-contrast, (B) post contrast, (C,D) axial and coronal CT bone window images showing well defined, expansile, enhancing soft tissue density lesion with few bony trabeculations within seen involving right maxillary sinus extending into nasal cavity causing its near complete obliteration.

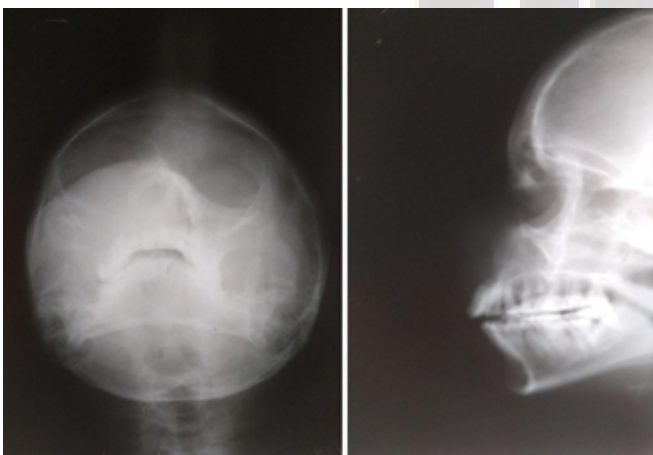


Figure 23: X-ray of para-nasal sinuses AP and lateral view showing well defined, fairly large, expansile, sclerotic lesion in right maxillary sinus extending into the nasal cavity and displacing nasal septum towards left side.

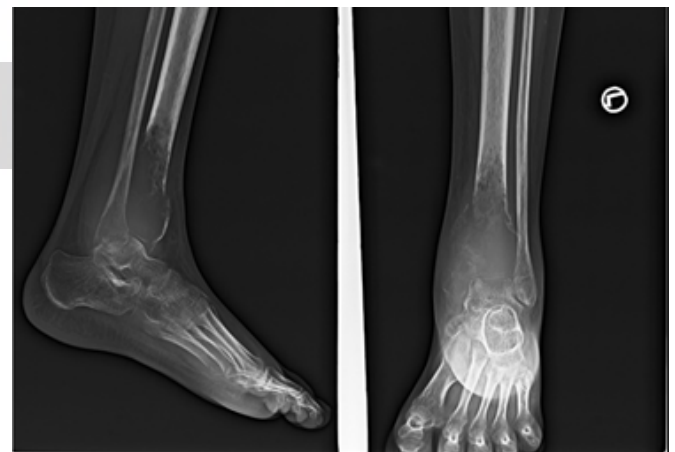
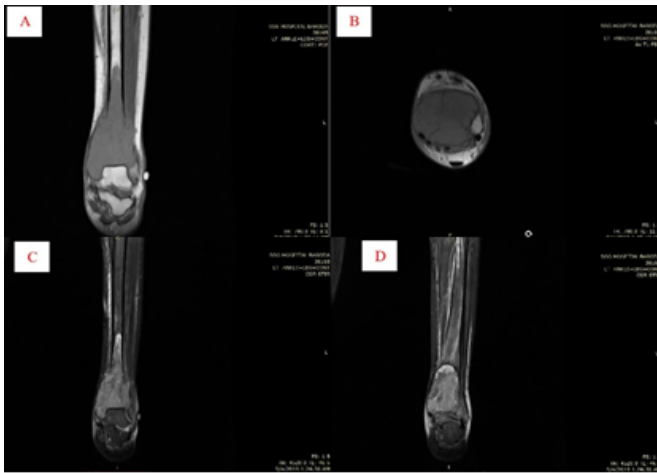


Figure 25: X-ray left ankle AP and lateral view showing large, expansile osteolytic lesion with wide zone of transition causing sever thinning or cortex and endosteal scalloping involving epimetaphysis of left distal tibia extending upto articular surface of distal tibia. Note the cortical break over proximal aspect of lesion. No visible matrix noted.



**Figure 26:** MRI of ankle with distal leg showing abnormal, expansile, large marrow signal intensity lesion- hypointense on T1 weighted images (A,B) heterogeneously hyperintense on STIR images (C,D). Note the adjacent soft tissue hyperintensity and hyperintensity on adjacent distal fibula (C,D). No evidence of pathological fracture.



**Figure 27:** (A) X ray left ankle AP and (B) lateral view showing large ill-defined mixed osteolytic and sclerotic lesion showing moth eaten pattern of destruction with osseous matrix and wide zone of transition involving distal tibia and extension of lesion into surrounding soft tissue.

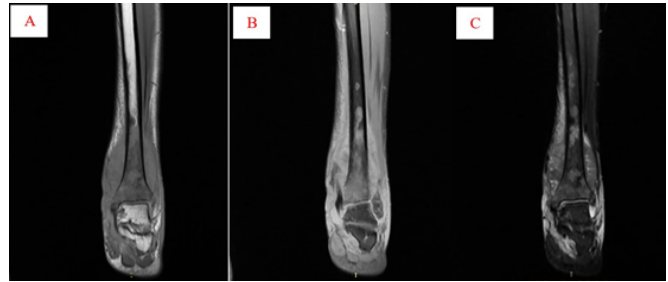


**Figure 28:** (A) coronal T1 weighted MR image the lesion appears heterogeneously hypointense and (B) coronal T1 weighted fat saturated post contrast image it shows heterogeneous enhancement, on (C) coronal STIR it appear hyperintense . Note the enhancing skip lesion in diaphysis of tibia.

**Histopathologic diagnosis:** Osteosarcoma

**Case 18:** A 50 years old male with c/o swelling over anterior chest wall.

**Radiologic diagnosis:** Multiple myeloma, Metastasis

**Histopathologic diagnosis:** Multiple myeloma

Metastasis commonly involve vertebral pedicles rather than vertebral bodies. It rarely involve mandible. [4]

**Case 19:** A 15 years female with c/o pain and swelling over right elbow. No history of trauma.

**Radiologic differential diagnosis:** Ewing sarcoma, Osteomyelitis, Langerhance cell histiocytosis

**Histopathologic diagnosis:** Ewing sarcoma

In case of ewing sarcoma a large extraosseous mass with permeative pattern of bone destruction. Fat plane is typically displaced and well defined. [2]

In case of osteomyelitis soft tissue abscess simulate extraosseous tumour. Intramuscular fat planes are typically poorly defined. [2] Patient usually presents within 4 weeks. [3]

In case of LCH soft tissue changes are reported however in soft tissue disease is more extensive in Ewing's sarcoma. [2]

**Conclusion**

Age of the patient and the clinical history is very crucial in drawing a reasonable diagnosis of a bone lesion. Most benign lesions are clinically asymptomatic and detected incidentally after a history of fresh trauma; while malignant lesions are having symptoms of local pain and swelling.

Plain radiography is first line imaging modality to detect and characterize a bone lesion; and to draw reasonable differential diagnosis.

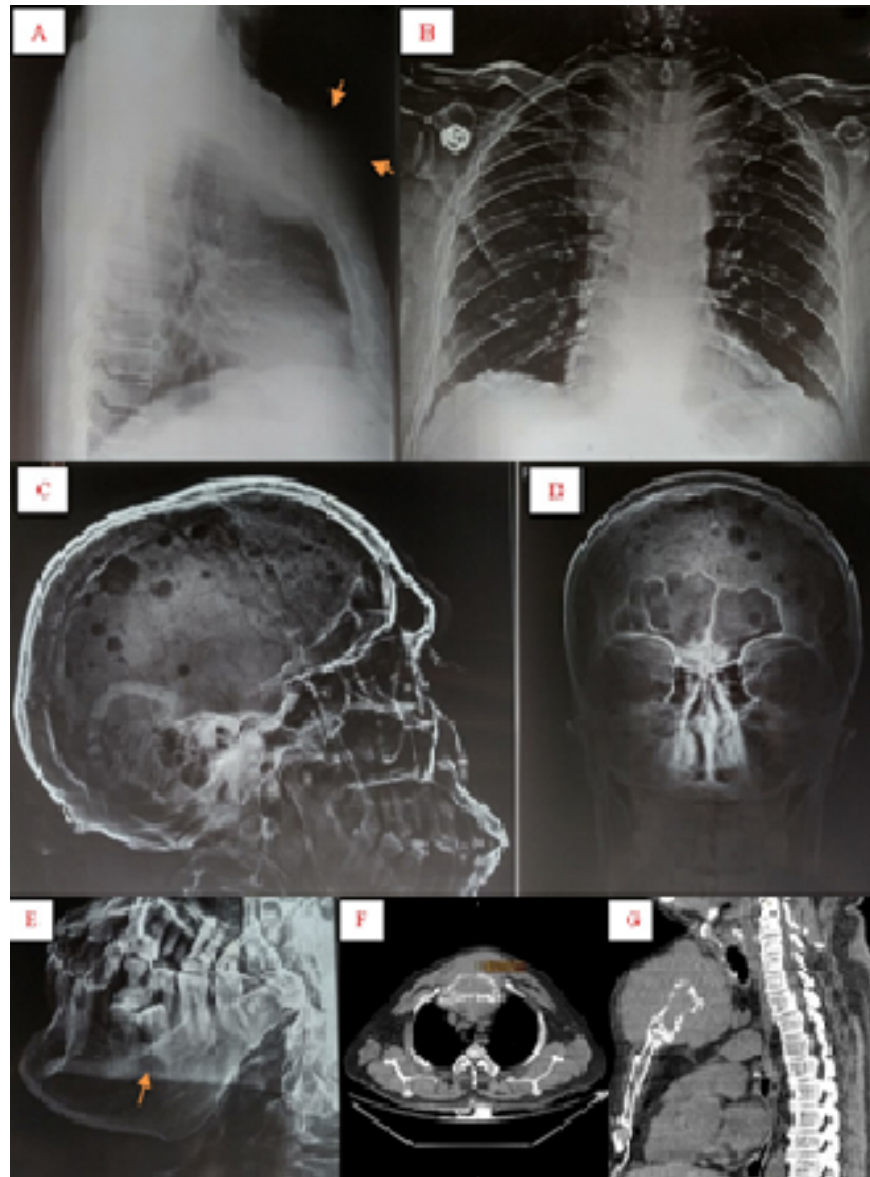


Figure 29: (A,B) X-ray chest AP and lateral view showing ill-defined osteolytic lesion with wide zone of transition involving manubrium of sternum. Note the extension of lesion into anterior chest wall in subcutaneous plane and into the anterior mediastinum. (C,D) X-ray skull AP and lateral views showing multiple variable sized punched out osteolytic lesions involving calvarium. (E) X-ray mandible lateral view showing ill-defined osteolytic lesion in body region (orange arrow). (F) Plain CT axial and (G) sagittal images showing soft tissue density lesion in sternum with destruction of cortex and extension of lesion into anterior mediastinum.

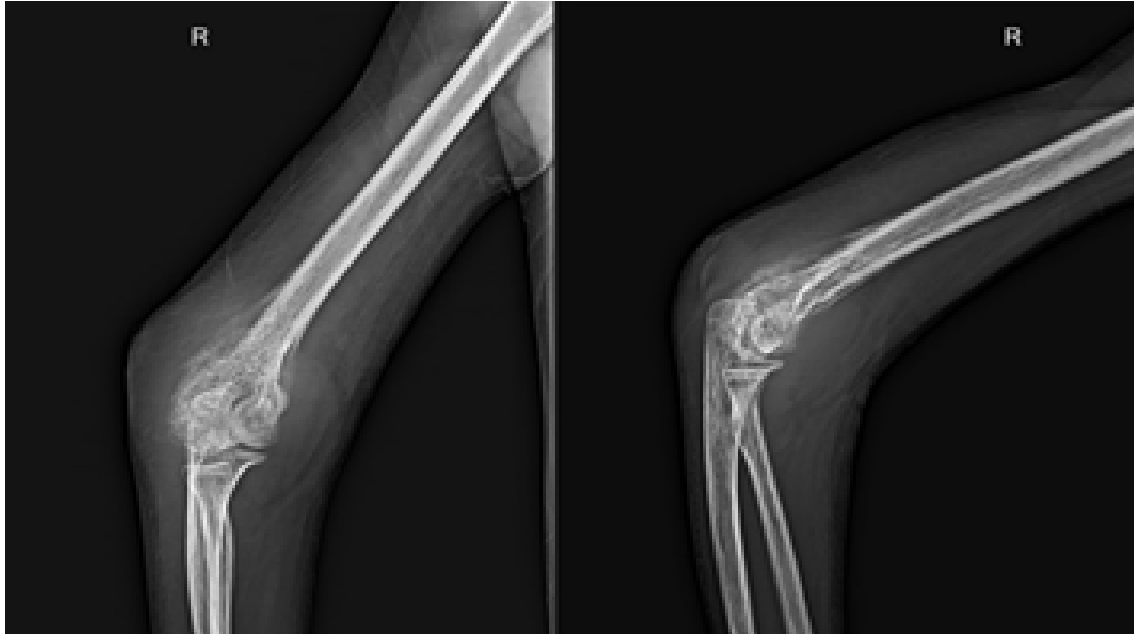


Figure 30: X ray elbow AP and lateral view showing ill-defined permeative pattern of osteolytic destruction with wide zone of transition with onion skin type of periosteal reaction involving epi-meta-diaphysis of distal humerus. Associated soft tissue swelling around elbow.

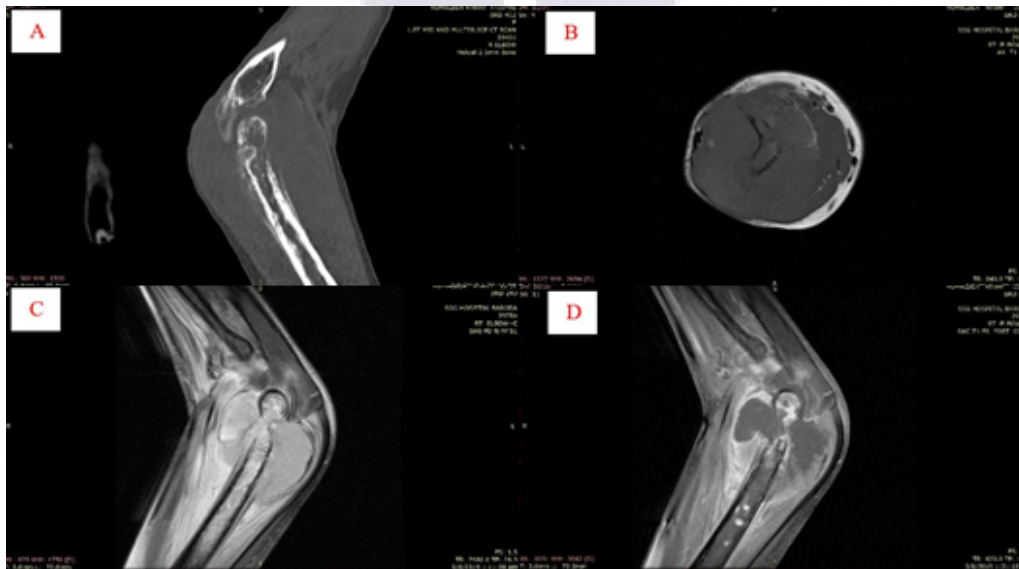


Figure 31: (A) sagittal CT image bone window showing ill-defined osteolytic lesion with wide zone of transition with onion skin type of periosteal reaction involving epi-meta-diaphysis of distal humerus. (B) Axial T1 weighted MR image it appear hypointense, on (C) sagittal PDFS image it appears heterogeneously hyperintense with adjacent muscle hyperintensity. (D) Sagittal T1 post contrast fat saturated image it shows moderate peripheral enhancement. Note the central non enhancing necrotic area and enhancing skip lesions within bone marrow (D).

CT is more sensitive than conventional radiography in detecting mineralization within the tumour matrix and pathological fracture. In areas of complex anatomy such as spine, scapula, skull and paranasal sinuses, CT was better than conventional radiography in demonstrating the lesion.

MRI is best investigation for detection of marrow infiltration, skip lesions and extension into the soft tissue.

## References

1. Miller TT. Bone tumors and tumor like conditions: analysis with conventional radiography. *Radiology*. 2008;246(3):662–74. Available from: <https://doi.org/10.1148/radiol.2463061038>.
2. Donnell PO. Evaluation of focal bone lesions: basic principles and clinical scenarios. *Imaging*. 2003;15:298–323. Available from: <https://doi.org/10.1259/img.15.4.150298>.
3. Nascimento D, Suchard G, Hatem M, de Abreu A. The role of magnetic resonance imaging in the evaluation of bone tumours and tumour-like lesions. *Insights Imaging*. 2014;5(4):419–440. Available from: <https://dx.doi.org/10.1007/s13244-014-0339-z>.
4. Yochum AM, Reckelhoff K, Kaeser M, Kettner NW. Ultrasonography and Radiography to Identify Early Post Traumatic Myositis Ossificans in an 18-Year-Old Male: A Case Report. *J Chiropr Med*. 2014;13(2):134–138. Available from: <https://dx.doi.org/10.1016/j.jcm.2014.06.004>.
5. Miller TT. Bone tumors and tumorlike conditions: analysis with conventional radiography. *Radiology*. 2008;246(3):662–674. Available from: <https://doi.org/10.1148/radiol.2463061038>.
6. Oba M, Inaba Y, Machida J, Saito T. Giant cell tumour of the femur in a 9-year-old girl, resulting in severe leg length discrepancy. *BMJ Case Rep*. 2016;2016:1–4. Available from: <https://dx.doi.org/10.1136/bcr-2015-214265>.
7. Wilson AJ, Kyriakos M, Ackerman LV. Chondromyxoid fibroma: radiographic appearance in 38 cases and in a review of the literature. *Radiology*. 1991;179(2):513–518. Available from: <https://dx.doi.org/10.1148/radiology.179.2.2014302>.
8. Hamada T, Ito H, Araki Y, Fujii K, Inoue M, Ishida O. Benign fibrous histiocytoma of the femur: review of three cases. *Skeletal Radiol*. 1996;25(1):25–29. Available from: <https://dx.doi.org/10.1007/s002560050027>.
9. Morán LM, Moeinvaziri M, Fernández A, Sánchez R. Multiple brown tumors mistaken for bone metastases. Computed tomography imaging findings. *ESRN*. 2016;47(2):537–541. Available from: <https://dx.doi.org/10.1016/j.ejrm.2016.03.001>.
10. Park JA, Moon SG, Kim NR. Benign Fibrous Histiocytoma with Cystic Change of the Femur: a Case Report. *Magn Reson Imaging*. 2016;20(4):264–272. Available from: <https://doi.org/10.13104/IMRI.2016.20.4.264>.
11. Scholl RJ, Kellett HM, Neumann DP, Lurie AG. Cysts and Cystic Lesions of the Mandible: Clinical and Radiologic-Histopathologic Review. *Radio Graphics*. 1999;19(5):1107–1124. Available from: <https://dx.doi.org/10.1148/radiographics.19.5.g99se021107>.

**Copyright:** © the author(s), 2020. It is an open-access article distributed under the terms of the Creative Commons Attribution License (CC BY 4.0), which permits authors to retain ownership of the copyright for their content, and allow anyone to download, reuse, reprint, modify, distribute and/or copy the content as long as the original authors and source are cited.

**How to cite this article:** Vatukiya SK, Kapadia B. Radioimaging Evaluation of Primary Bone Tumors and Tumor like Lesions. *Asian J. Med. Radiol. Res.* 2020;8(1):69-82.

DOI: [dx.doi.org/10.47009/ajmrr.2020.8.1.14](https://dx.doi.org/10.47009/ajmrr.2020.8.1.14)

**Source of Support:** Nil, **Conflict of Interest:** None declared.